# Appendix for

## Identification and validation of serum metabolite biomarkers for endometrial cancer diagnosis

Wanshan Liu†, Jinglan Ma†, Juxiang Zhang, Jing Cao, Xiaoxiao Hu, Yida Huang, Ruimin Wang, Jiao Wu, Wen Di*, Kun Qian*, Xia Yin*

*Correspondence author. Email: diwen@renji.com, k.qian@sjtu.edu.cn, yinxia@renji.com

†These authors contributed equally to this work

**Table of contents**

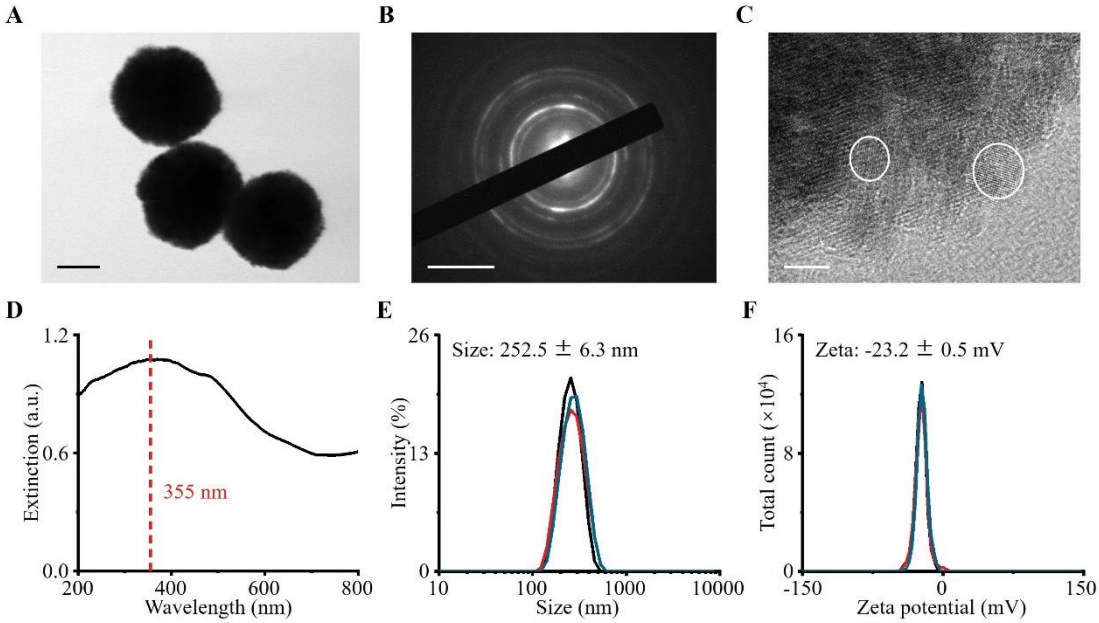


**Appendix Figure S1. Characterization of the ferric oxide particles.**

**A, B. (A)** Transmission electron microscopy (TEM) image (scale bar = 100 nm) and **(B)** selected area electron diffraction (SAED) pattern (scale bar = 5 $nm^{-1}$) of the ferric oxide particles.

**C.** High-resolution TEM (HRTEM) image displayed the crystal lattice of the ferric oxide particles, marked by white circles. The scale bar was 5 nm.

**D.** Ultraviolet-visible (UV-Vis) spectrum of the ferric oxide particles showed a strong absorbance at 355 nm.

**E, F. (E)** Dynamic light scattering (DLS) and **(F)** zeta potential were recorded by 3 independent technical replicates. Data were mean ± SD, $N = 3$ technical replicates.

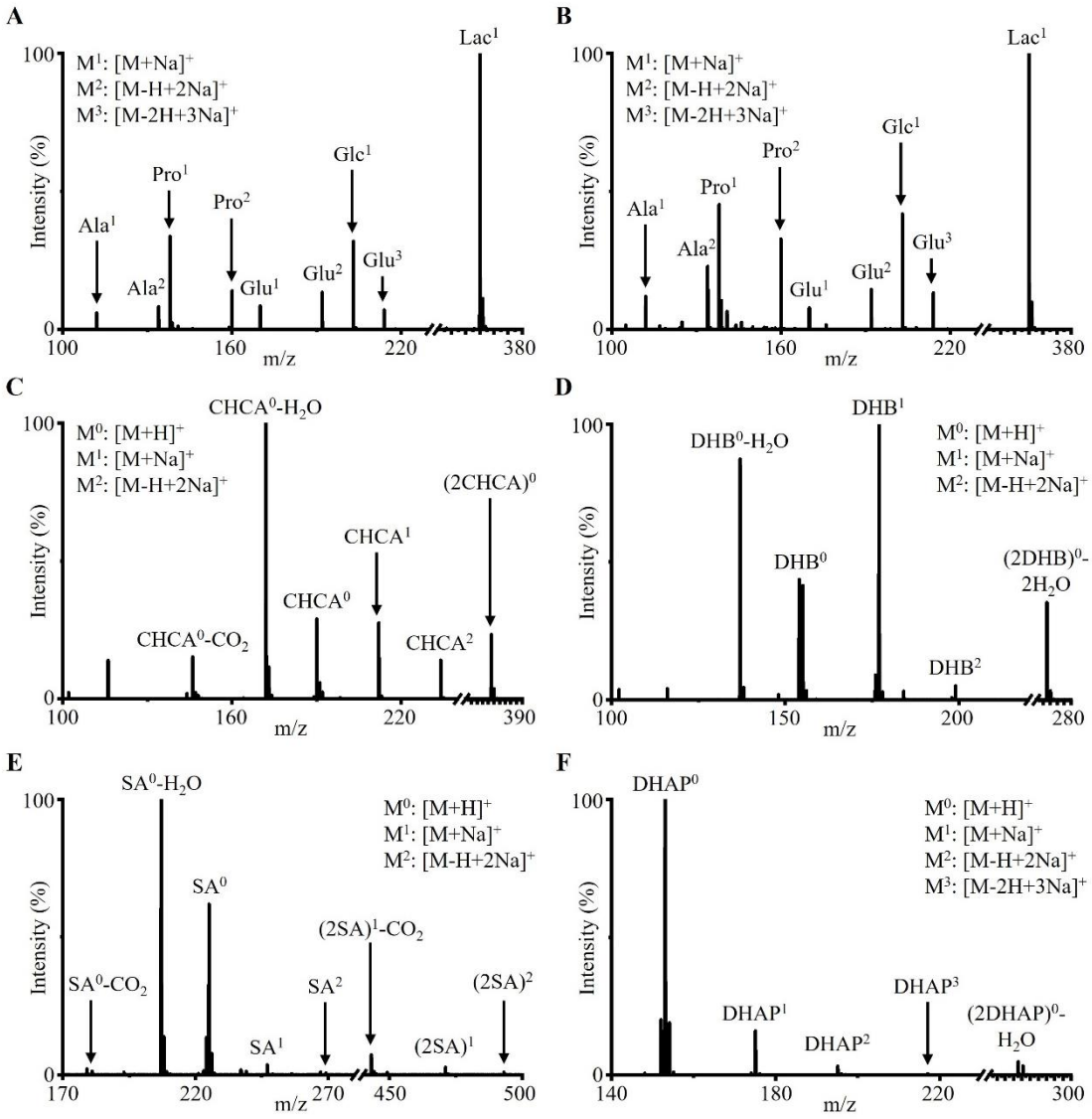


**Appendix Figure S2. High salt and protein tolerance of PELDI-MS.**

**A, B.** Typical mass spectrum of the standard sample under **(A)** high salt condition (20 mM $Na^+$) and **(B)** biofluid-mimic condition (20 mM $Na^+$ and 10 mg/mL protein) using ferric oxide particles. Alkali metal cation adduction ($[M+Na]^+$, $[M-H+2Na]^+$, and $[M-2H+3Na]^+$) of small metabolites (alaline (Ala), proline (Pro), glutamic acid (Glu), glucose (Glc), and lactose (Lac)) was marked.

**C-F.** Typical mass spectra of the standard sample under high salt condition (20 mM $Na^+$) using **(C)** α-cyano-4-hydroxycinnamic acid (CHCA), **(D)** 2,5-dihydroxybenzoic acid (DHB), **(E)** sinapic acid (SA), and **(F)** 2,6-dihydroxyacetophenone (DHAP).

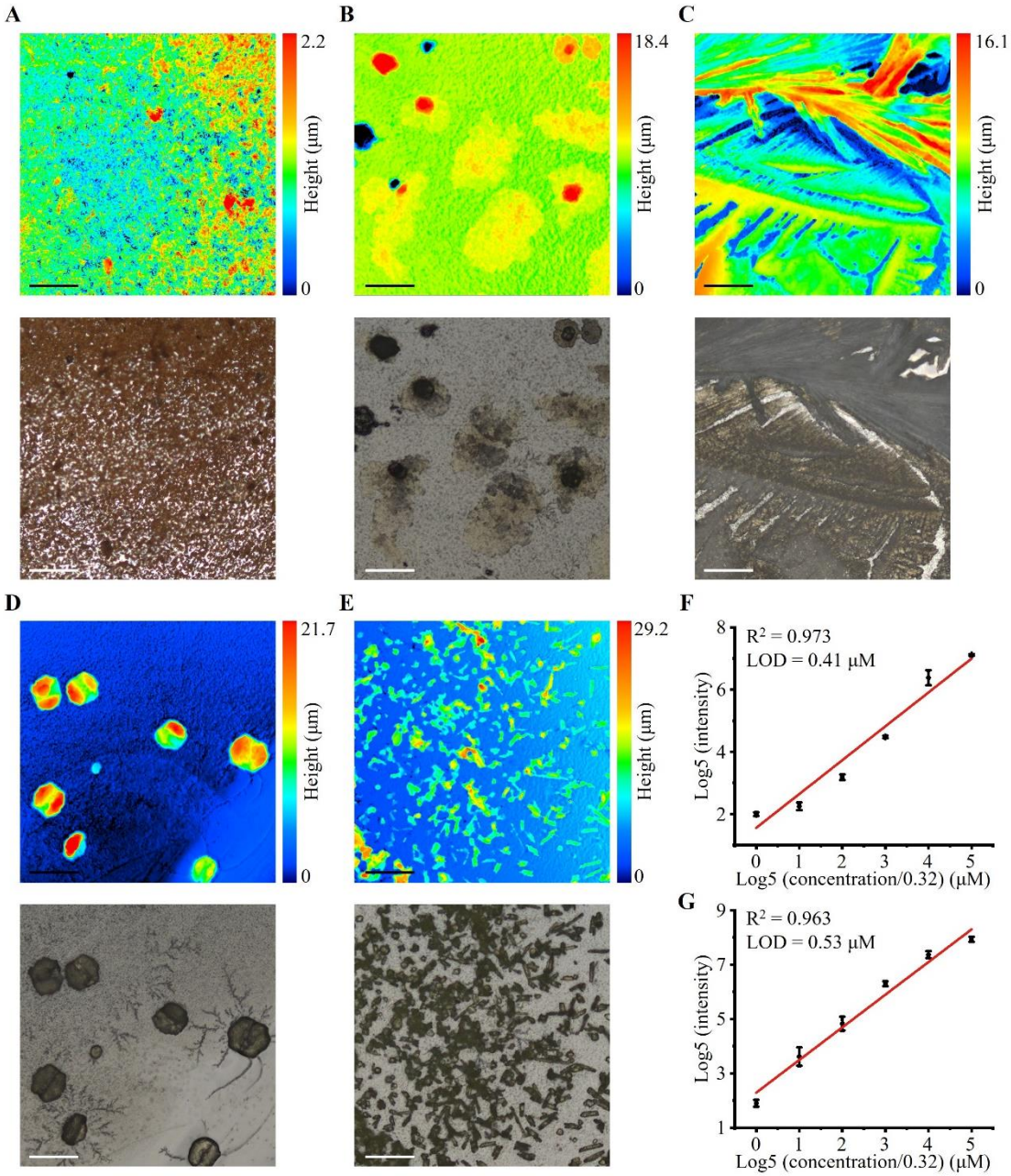


**Appendix Figure S3. High reproducibility and good linear response of PELDI-MS.**

**A-E.** 3D confocal reconstruction images displayed the homogeneous co-crystallization of **(A)** ferric oxide particles and heterogeneous co-crystallization of **(B)** CHCA, **(C)** DHB, **(D)** SA, and **(E)** DHAP. The scale bars were 100 μm.

**F, G.** The PELDI-MS offered a good linear response ($R^2$ = 0.963-0.973) with a limit of detection (LOD) of 0.41-0.53 μM in **(F)** alanine and **(G)** glucose analysis. Data were mean ± SD, $N$ = 3 technical replicates.

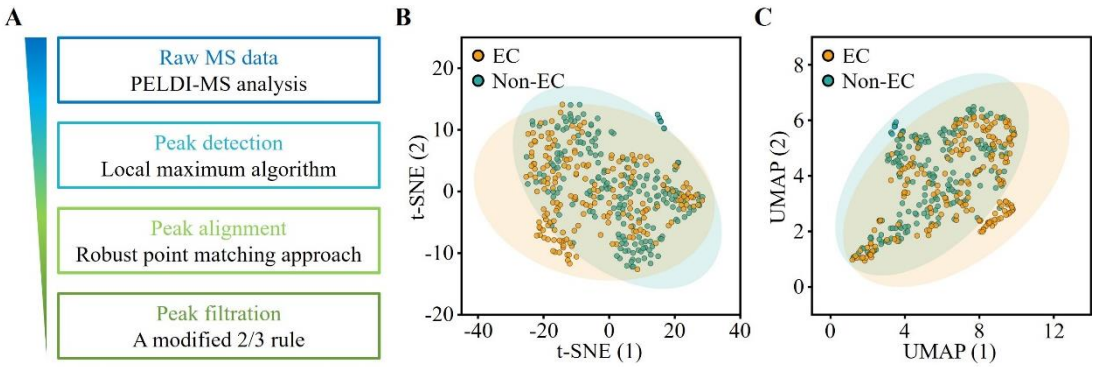


**Appendix Figure S4. Data processing and SMFs Characterization of EC and Non-EC.**

**A.** Data processing of native m/z signals, including peak detection using a local maximum algorithm, peak alignment using a robust point matching approach, and peak filtration employing a modified 2/3 rule.

**B, C.** The unsupervised analysis of **(B)** t-distributed stochastic neighbor embedding (t-SNE) and **(C)** uniform manifold approximation and projection (UMAP) of SMFs showed a certain degree of overlap between EC and Non-EC groups.

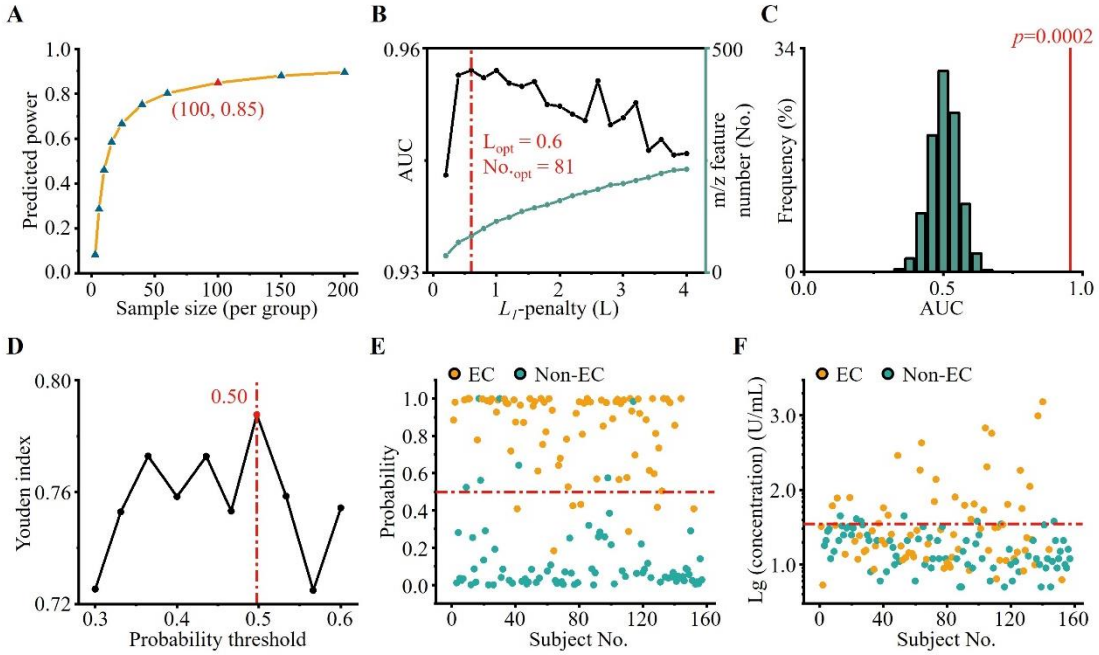


**Appendix Figure S5. Machine learning of SMFs for EC diagnosis.**

**A.** SMFs of 12 samples (6 EC and 6 Non-EC) were included in a preliminary study to determine the sample number required for statistically significant machine learning.

**B.** Optimization of the $L_1$-penalty for LASSO model in the discovery cohort. The optimized $L_1$-penalty ($L_{opt}$ = 0.6) and m/z feature number ($No._{opt}$ = 81) were marked with a red dashed line.

**C.** The permutation test with 5000 randoms confirmed no overfitting of LASSO model.

**D.** Optimization of the probability threshold for SMFs with LASSO model using Youden index, and the maximum Youden index was obtained at the optimal probability threshold of 0.50.

**E.** Probability generated by machine learning for EC diagnosis, using LASSO as an example, for subjects (EC in orange dots, Non-EC in cyan dots) in the independent validation cohort.

**F.** The concentration of CA-125 for subjects (EC in orange dots, Non-EC in cyan dots) tested in clinics in the independent validation cohort.

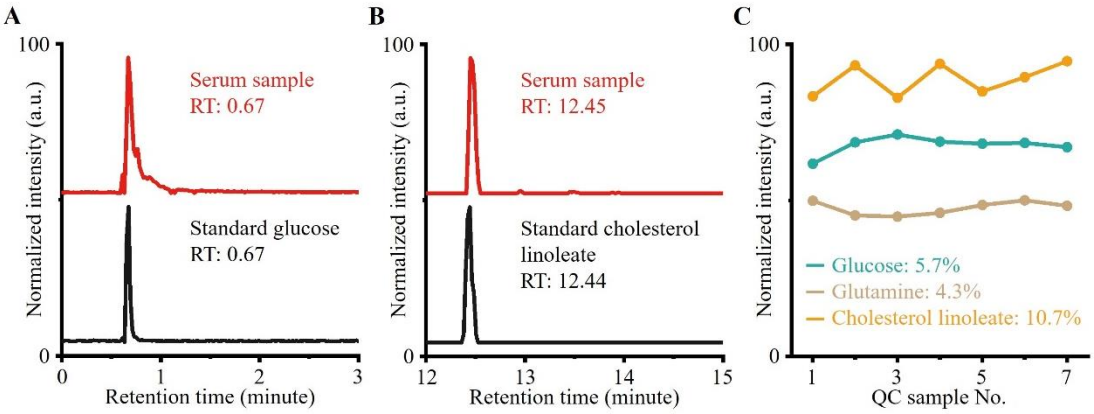


**Appendix Figure S6. Metabolic biomarker panel validation in UPLC-MS.**

**A, B.** Chromatograms of standard **(A)** glucose and **(B)** cholesterol linoleate with serum samples confirmed the reliability of metabolite detection in UPLC-MS validation.

**C.** Intensities of metabolites (glutamine, glucose, and cholesterol linoleate) in 7 QC samples, showing 4.3-10.7% CVs during detection in UPLC-MS validation.

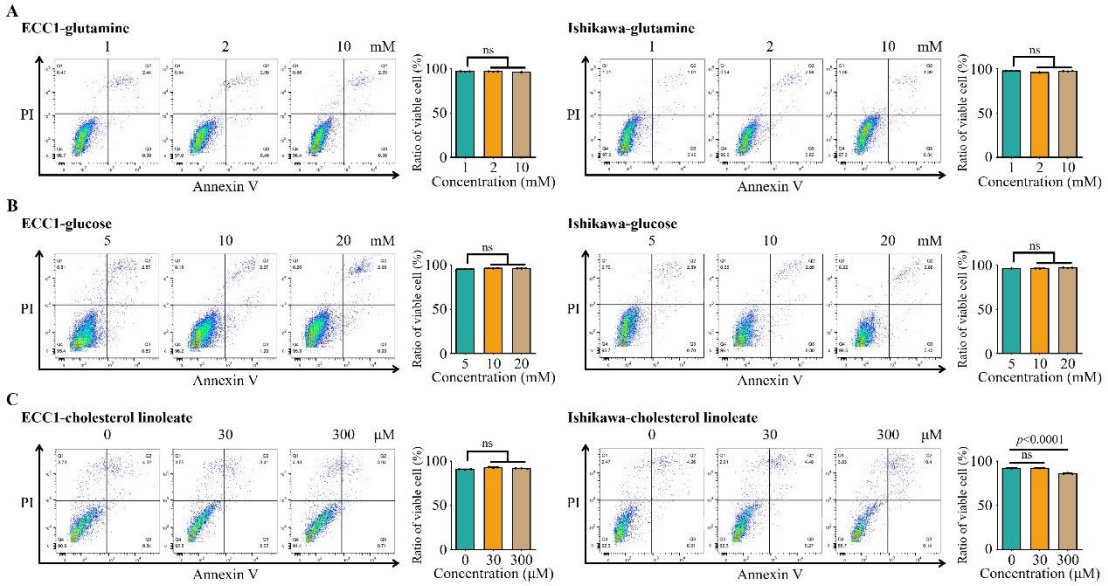


**Appendix Figure S7. Apoptotic impacts of biomarkers on EC cell lines.**

**A, B. (A)** Glutamine and **(B)** glucose did not affect the apoptosis process in EC cell lines.

**C.** Cholesterol linoleate induced apoptosis in Ishikawa cells at 300 μM, while demonstrating no influence on ECC1 cells. Cell apoptosis was examined by flow cytometric analysis. Data were mean ± SD, $N = 3$ biological replicates, one-way ANOVA, ns (no significance, $p > 0.05$).

**Appendix Table S1.** Peak intensities of metabolites for the standard sample under high salt (20 mM $Na^+$) and biofluid-mimicking conditions (20 mM $Na^+$ and 10 mg/mL protein) using different matrices (particles (Par), CHCA, DHB, SA, and DHAP).

| Condition | Matrix | Alanine | Proline | Glutamic acid | Glucose | Lactose | Sum [a)] |
|---|---|---|---|---|---|---|---|
| 20 mM of $Na^+$ | Par | 28494 | 95042 | 58029 | 63222 | 198034 | 442821 |
| | CHCA | 10 | 3892 | 1080 | 27 | 717 | 5726 |
| | DHB | 4 | 643 | 144 | 9 | 19 | 819 |
| | SA | 21 | 94 | 46 | 248 | 46 | 457 |
| | DHAP | 37 | 5768 | 491 | 25 | 1253 | 7575 |
| 20 mM of $Na^+$ and 10 mg/mL of protein | Par | 49196 | 110063 | 50314 | 59035 | 140708 | 409316 |
| | CHCA | 147 | 515 | 243 | 230 | 750 | 1886 |
| | DHB | 30 | 5492 | 728 | 387 | 3315 | 9952 |
| | SA | 27 | 72 | 45 | 30 | 28 | 201 |
| | DHAP | 76 | 4459 | 623 | 25 | 2469 | 7652 |

a) The sum of peak intensities for alanine, proline, glutamic acid, glucose, and lactose in the standard sample under high salt (20 mM $Na^+$) and biofluid-mimicking conditions (20 mM $Na^+$ and 10 mg/mL protein) using different matrice.

**Appendix Table S2.** Coefficient of variation of m/z feature intensity for metabolites in the standard metabolite mixture.

| Metabolite | Adduct | m/z | S.D. [a)] | Mean [a)] | CV [a)] |
|---|---|---|---|---|---|
| Alanine | $[M+Na]^+$ | 112.04 | 3295.69 | 49476.60 | 6.7% |
| | $[M-H+2Na]^+$ | 134.02 | 7328.40 | 99288.59 | 7.4% |
| Proline | $[M+Na]^+$ | 138.05 | 14092.60 | 230216.68 | 6.1% |
| | $[M-H+2Na]^+$ | 160.03 | 12120.18 | 150915.40 | 8.0% |
| Glutamic acid | $[M+Na]^+$ | 170.04 | 6357.95 | 65004.86 | 9.8% |
| | $[M-H+2Na]^+$ | 192.02 | 11973.21 | 114683.39 | 10.4% |
| | $[M-2H+3Na]^+$ | 214.01 | 8177.93 | 74248.67 | 11.0% |
| Glucose | $[M+Na]^+$ | 203.05 | 12607.42 | 196665.75 | 6.4% |
| Lactose | $[M+Na]^+$ | 365.11 | 19907.40 | 358524.07 | 5.6% |

a) The standard deviation (S.D.), mean, and coeffitient of variance (CV) were calculated based on 16 independent replicates.

**Appendix Table S3.** Clinical characteristics of the enrolled EC and Non-EC subjects.

| Characteristic | EC [a)] | Non-EC [a)] | *p* value |
|---|---|---|---|
| **Sample number** | 191 | 204 | – |
| **Age (year)** | | | |
| Mean (range) | 58 (27-81) | 43 (17-79) | < 0.001 |
| **CA-125** [b)] | | | |
| Mean (range) | 137 (4-3201) | 20 (2-82) | < 0.001 |
| **BMI** | | | |
| Mean (range) | 25 (17-46) | 23 (15-34) | < 0.001 |
| **Diabetes** | | | |
| (No/Yes/Unknown) | 149/37/5 | 188/16/0 | < 0.001 |
| **Menopause** | | | |
| (No/Yes/Unknown) | 61/125/5 | 164/40/0 | < 0.001 |
| **Hypertension** | | | |
| (No/Yes/Unknown) | 131/56/4 | 158/46/0 | 0.11 |
| **FIGO Stage (%)** [c)] | | | |
| I | 126 (66.0) | – | – |
| II | 8 (4.2) | – | – |
| III | 34 (17.8) | – | – |
| IV | 13 (6.8) | – | – |
| Recurrence | 10 (5.2) | – | – |
| **Histology (%)** | Endometrioid 169 (88.5) | Polyp/Polypoid 151 (74.0) | – |
| | Serous 19 (9.9) | Hyperplasia 42 (20.6) | – |
| | Clear cell 3 (1.6) | Adhesions 11 (5.4) | – |

a) The EC and Non-EC subjects were diagnosed by two experienced pathologists independently, based on pathological examination.

b) The concentration of CA-125 (U/mL) for EC and Non-EC subjects was assessed in the clinical setting.

c) The stage information of EC was determined according to the FIGO 2018 standard.

**Appendix Table S4.** Performance of the 5 machine learning algorithms for EC diagnosis in the discovery cohort.

| Algorithm | AUC [a)] | 95% CI [a)] | *p* value |
|---|---|---|---|
| LASSO | 0.957 | 0.906-1.000 | – |
| Logistic regression | 0.940 | 0.876-0.998 | < 0.001 |
| PLS-DA | 0.940 | 0.877-0.996 | < 0.001 |
| Random forest | 0.905 | 0.822-0.986 | < 0.001 |
| Decision tree | 0.757 | 0.635-0.879 | < 0.001 |

a) The area-under-the-curve (AUC) and corresponding 95% confidence interval (CI) were calculated in the discovery cohort.

**Appendix Table S5.** Sensitivity and specificity of the SMFs and CA-125 for EC diagnosis and early-stage (FIGO 2018 stage I/II) EC diagnosis in both the discovery and validation cohorts.

| | Diagnostic approach [a)] | Cohort | Sensitivity | Specificity |
|---|---|---|---|---|
| **Diagnosis** | SMFs | Discovery | 86.1% | 91.9% |
| | | Validation | 90.8% | 91.4% |
| | CA-125 | Discovery | 37.4% | 74.8% |
| | | Validation | 32.9% | 91.4% |
| **Early diagnosis** | SMFs | Discovery | 85.7% | 91.9% |
| | | Validation | 91.2% | 91.4% |
| | CA-125 | Discovery | 22.1% | 74.8% |
| | | Validation | 26.3% | 91.4% |

a) The sensitivity and specificity were calculated based on the SMFs (272 m/z features) with LASSO model or the concentration of CA-125 in serum.

**Appendix Table S6.** The information of identified biomarkers for the differentiation of EC and Non-EC.

| Measured m/z [a)] | Error (ppm) [b)] | Molecular formula [c)] | Metabolite [d)] | Adduct [c)] | HMDB ID [d)] |
|---|---|---|---|---|---|
| 212.957 | \ | \ | \ | \ | \ |
| 203.052 | -1.37 | $C_6H_{12}O_6$ | Glucose | $[M+Na]^+$ | HMDB0000122 |
| 204.056* | -1.52 | | | $[M+Na]^+$ | |
| 219.026 | -2.31 | | | $[M+K]^+$ | |
| 222.988 | -0.86 | $C_5H_{10}N_2O_3$ | Glutamine | $[M-H+2K]^+$ | HMDB0000641 |
| 671.575 | 2.59 | $C_{45}H_{76}O_2$ | Cholesterol linoleate | $[M+Na]^+$ | HMDB0000610 |
| 672.579* | 2.69 | | | $[M+Na]^+$ | |

a) The accurate m/z value was measured using the FT-ICR-MS with high resolution, and the * referred to the relevant ions of isotopes.

b) The error of measured m/z was calculated as (measured m/z - theoretical m/z) / theoretical m/z.

c) The molecular formula and adduct species were annotated based on accurate m/z measurements (< 3 ppm).

d) The metabolite name and HMDB ID were searched in HMDB based on the molecular formula.

**Appendix Table S7.** Odds ratio of Met-score and potentially relevant variables (Age, BMI, diabetes, and menopause).

| Covariate | Odds ratio (95% CI) | Significance (*p* value) |
|---|---|---|
| **Met-score** | 7.356 (5.924-9.143) | < 0.001 |
| **Age** | 3.357 (2.465-4.572) | < 0.001 |
| **BMI** | 1.158 (0.973-1.379) | 0.397 |
| **Diabetes** | 0.394 (0.240-0.645) | 0.059 |
| **Menopause** | 1.241 (0.752-2.048) | 0.666 |